

A shrinking model for combustion/gasification of char based on transport and reaction time scales

B. Peters*, **A. Džiugys****, **R. Navakas*****

**Université du Luxembourg, Campus Kirchberg, 6, rue Coudenhove-Kalergi, L-1359 Luxembourg,*

E-mail: bernhard.peters@uni.lu

***Lithuanian Energy Institute, Breslaujos g. 3, LT-44403 Kaunas, Lithuania, E-mail: dziugys@mail.lei.lt*

****Lithuanian Energy Institute, Breslaujos g. 3, LT-44403 Kaunas, Lithuania, E-mail: rnavakas@mail.lei.lt*

crossref <http://dx.doi.org/10.5755/j01.mech.18.2.1564>

1. Introduction

Biomass is considered as an alternative source of energy, because thermal conversion of biomass allows for a reduction of net carbon dioxide (CO₂) [1-4]. If biomass is locally available [2], it is also favourable from an economical point of view. However, thermal conversion of biomass and coal as major represents of solid fuels is a complex process involving a variety of aspects from chemistry and physics. Modelling efforts of several researchers [5-11] include one-dimensional differential conservation equations in a steady state or transient formulation. This approach may be sufficient to describe accurately drying or pyrolysis of solid fuel, however, may lack accuracy during gasification when shrinking of a particle occurs. Shrinkage affects significantly heat and mass transfer due to a decreasing surface. Furthermore, a shrinking particle causes heat and mass to reach its centre at a faster rate due to smaller dimensions.

Maa and Bailie [12] are believed to be the first to employ a shrinking core model to describe pyrolysis of cellulose. The model distinguishes into an unreacted core and an inert outer layer of pyrolysed char. A pyrolysis reaction is assumed to occur at the interface between the char and the unreacted inner layer and is described by an Arrhenius first-order decomposition. Conservation of energy is applied to solve for temperature distribution.

Villermaux et al. [13] developed a simplified model without internal flow for pyrolysis of wood that includes a single first order reaction to account for combustion. The latter representing depletion of wood was employed to estimate shrinkage. While they considered wood as a homogeneous particle, Parker [14] assumed a wooden particle to be composed of cellulose, hemicellulose and lignin. Conversion was described by individual reaction rates for each component. The kinetic parameters were extracted from experiments. The particle is divided into a region of virgin wood and char that extends into the depth of the particle by 10% of the initial particle mass. Surface recession takes place in the char layer, whereby the total area of the char region is defined by experimental contraction coefficients parallel and normal to the surface. Similar to the model of Villermaux et al. [13] internal flow of moisture and volatiles was neglected.

Saastamoinen and Richard [15] obtained the total period of combustion for their shrinking core approach as a sum of kinetic and transport limited approaches for the reaction rate. A similar concept was employed by Ragland et al. [16], who considered mass transfer as the rate limit-

ing process for chunkwood. Hence, the shrinking rate of the wood particle is directly correlated to the mass transfer e.g. flow conditions. This approach was extended by Ouedraogo et al. [17] to describe combustion of chunkwood and wood particles by a shrinking core model. They included appropriate mass transfer coefficients, the effect of moisture content and a quasisteady thermal balance equation for char and core region. Their findings indicate that increasing moisture content reduces the burning rate and appropriate mass transfer coefficients were derived for different flow conditions including blowing.

Di Blasi [18] extended these approaches by a primary and secondary pyrolysis scheme and variable solid densities. Shrinkage is defined as a function of three parameters. The volume of the solid decreases linearly with the depletion of wood mass and increases with the char formed multiplied by the shrinkage factor. Results predicted by this model indicate that the pyrolysis time reduces and changes the product yield. Thus, it highlights the need for modelling of shrinkage during thermal conversion of solid fuels. However, no experimental values were available for the parameters.

Hagge et al. [19] presented in their study experimental data for the shrinkage parameters in conjunction with a detailed pyrolysis model. It is based on conservation equations for mass, momentum, species and energy. The particle consists of wood, char and various gas species due to pyrolysis. Shrinkage is assumed to vary linearly with the composition of the particle during pyrolysis. Their approach was validated by the experimental work of Tran and White [20] including their shrinkage factor. Predicted results show that shrinkage had a negligible effect on pyrolysis times and product yield for both thermally thin ($Bi < 0.2$) and thick ($0.2 < Bi < 10$) particles, where Bi is Biot number. Only in the thermal wave regime ($Bi > 10$) both pyrolysis period and yield changed significantly.

2. Numerical approach

A particle is considered to consist of different phases: gas, liquid, solid, inert, where the inert, solid and liquid species are considered as immobile. The gas phase fills the voids in the porous structure, and is assumed to behave as an ideal gas. Each of the phases may undergo various conversion by homogeneous, heterogeneous or intrinsic reactions whereby the products may experience a phase change such as encountered during drying, i.e., evaporation. The need for heterogeneous reactions was pointed out by Chapman [21], while intrinsic rate model-

ling was emphasised by Rogers et al. [22] and Hellwig [23] to capture accurately the nature of various reaction processes.

Furthermore, local thermal equilibrium between the phases is assumed. It is based on the assessment of the ratio of heat transfer by conduction to the rate of heat transfer by convection expressed by the Peclet number as described by Peters [10] and Kansa et al. [24]. According to Man and Byeong [25], one-dimensional differential conservation equations for mass, momentum and energy are sufficiently accurate. The importance of a transient behaviour is stressed by Lee et al. [26, 27]. Transport through diffusion has to be augmented by convection as stated by Rattea et al. [28] and Chan et al. [6]. In general, the inertial term of the momentum equation is negligible due to a small pore diameter and a low Reynolds number [24]. However, for generality, the inertial terms may be taken into account by the current formulation.

Thus, the Discrete Particle Model (DPM) offers a high level of detailed information and, therefore, is assumed to omit empirical correlations, which makes it independent of particular experimental conditions for both a single particle and a packed bed of particles. Such a model covers a larger spectrum of validity than an integral approach and considerably contributes to the detailed understanding of the process [29-31]. The predictions include major properties such as temperature and species distribution inside a particle. Summarising, the following assumptions are made to describe conversion of a particle:

- a particle consists of a solid and a gaseous porous phase that may be accompanied by a liquid phase;
- particle's geometry is represented by slab, cylinder or sphere; description by one-dimensional and transient differential conservation equations for mass, momentum and energy; liquid, inert and solid species are considered to be immobile; ideal gas behaviour prevails in the pore space;
- thermal equilibrium between gaseous, liquid and solid phases inside a particle; diffusive transport dependent on porosity and tortuosity;
- space dependent average transport properties for diffusion and conduction inside a particle;
- convective transport in the gas phase through Darcy flow; thermal conversion described by homogeneous, heterogeneous and intrinsic rate modelling;
- surface recession of a particle during combustion and gasification processes.

Conservation of mass for the porous gas phase is expressed as follows:

$$\varepsilon \frac{\partial \rho_g}{\partial t} + \frac{1}{r^n} \frac{\partial}{\partial r} \left(r^n \rho_g \mathbf{v}_g \right) = S_{mass} \quad (1)$$

where ε , ρ , \mathbf{v} and S_{mass} denote porosity of the particle, gas density, velocity and mass sources due to a transfer between the solid/liquid phase to the gas phase and its reactions, respectively. Due to a general formulation of the conservation equation with the independent variable r as a characteristic dimension, the geometrical domain can be considered as a plate ($n = 0$), cylinder ($n = 1$) or sphere ($n = 2$).

Transport of gaseous species within the porous space of a particle is approximated by a Darcy flow. An

analysis of orders of the relevant terms yields [32] that convective terms are negligible and consequently the effect of friction is described by the Darcy and Forchheimer correlation. Hence, the following balance of linear momentum is applied

$$\varepsilon \frac{\partial \rho_g \mathbf{v}_g}{\partial t} = - \frac{\partial p}{\partial r} - \frac{\mu}{k} \mathbf{v}_g - C \rho_g \mathbf{v}_g |\mathbf{v}_g| \quad (2)$$

where p , μ , k and C stand for pressure, viscosity, permeability and Forchheimer coefficient, respectively. In general, the inertial terms may be neglected, however, are kept within the present formulation. The solution of the continuity and momentum equation furnishes a gas velocity and pressure distribution within the pore space of a particle.

Convection in conjunction with diffuse transport describes the distribution of gaseous species i in the porous particle versus time and space as follows

$$\begin{aligned} \frac{\partial \rho_{i,g}}{\partial t} + \frac{1}{r^n} \frac{\partial}{\partial r} \left(r^n \mathbf{v}_g \rho_{i,g} \right) &= \\ &= \frac{1}{r^n} \frac{\partial}{\partial r} \left(r^n \frac{D_{i,eff}}{M_i} \frac{\partial \rho_{i,g}}{\partial r} \right) + \sum_{k=1}^l \omega_{k,i,gas} \end{aligned} \quad (3)$$

where $\rho_{i,g}$ and $\omega_{k,i}$ are partial density of gaseous specie i and a reaction source. A contribution of the Knudsen diffusion is neglected due to an approximate value of pore diameters of $\sim 50.0 \mu\text{m}$ and a pressure of approximately 1.0 bar, so that only molecular diffusion in the pores is taken into account [9, 33]. As a result of the averaging process and the influence of tortuosity τ on diffusion, an effective diffusion coefficient is derived as $D_{i,eff} = D_i \varepsilon_p / \tau$ [34, 35], where ε_p is the porosity of the particle and the molecular diffusion coefficients D_i are taken from the equivalent ones of the appropriate species in air.

Similarly, conservation of both liquid and solid species are written as

$$\frac{\partial \rho_{i,liquid/solid}}{\partial t} = \sum_{k=1}^l \omega_{k,i,liquid/solid} \quad (4)$$

where the right hand side comprises all reactions k involving a specie i , each of which is characterised by specific kinetic parameters [36-39]. Due to resolved temperature and species distribution within a particle, reaction regimes [10] of a shrinking- and a reacting-core mode are distinguished. Depending on the rate-limiting process, the depletion of solid material therefore results in either a decreasing particle density or a reduction of particle size [10, 40].

Due to a negligible heat capacity of the gas phase compared to the liquid, inert and solid phase conservation of energy includes solids and liquids only (local thermal equilibrium)

$$\frac{\partial \left(\sum_{i=1}^k \rho_i c_{p,i} T \right)}{\partial t} = \frac{1}{r^n} \frac{\partial}{\partial r} \left(r^n \lambda_{eff} \frac{\partial T}{\partial r} \right) + \sum_{k=1}^l \dot{\omega}_k H_k \quad (5)$$

The locally varying conductivity λ_{eff} is evaluated as

$$\lambda_{eff} = \varepsilon_p \lambda_g + \sum_{i=1}^k \eta_i \lambda_{\tau,solid} + \lambda_{rad} \quad [33] \quad \text{which takes into account}$$

count heat transfer by conduction in the gas, solid, char and radiation in the pore. The latter is approximated as

$$\lambda_{rad} = 4.0 \frac{\varepsilon}{1-\varepsilon} \sigma T^3, \text{ where } \varepsilon, \sigma \text{ and } T \text{ stand for porosity, Boltzmann constant and temperature, respectively.}$$

The source term on the right hand side represents heat release or consumption due to chemical reactions.

In order to complete the mathematical formulation of the problem, initial and boundary conditions must be provided. A wide range of experimental work has already been carried out in this field and appropriate laws in terms of Nusselt and Sherwood numbers are well established for different geometries and flow conditions [29, 41-45]. The following boundary conditions at the particle surface (with particle radius R) for mass and heat transfer of a particle are applied

$$-\lambda_{eff} \left. \frac{\partial T}{\partial r} \right|_R = \alpha (T_R - T_\infty) + \dot{q} \quad (6)$$

$$-D_{i,eff} \left. \frac{\partial c_i}{\partial r} \right|_R = \beta_i (c_{i,R} - c_{i,\infty}) \quad (7)$$

where \dot{q} , T_∞ , $c_{i,\infty}$, α and β denote external heat flux, ambient gas temperature, concentration of specie i , heat and mass transfer coefficients, respectively. Due to the outflow \dot{m}_g of volatiles and steam from the particle, the Stefan correction is introduced into the transfer coefficients, which are estimated as follows [41]

$$\beta = \frac{\dot{m}_g / \rho_g}{\exp(\dot{m}_g / \rho_g \beta_0) - 1} \quad (8)$$

$$\alpha = \frac{\dot{m}_g c_{p,g}}{\exp(\dot{m}_g c_{p,g} / \alpha_0) - 1} \quad (9)$$

where α_0 and β_0 denote the transfer coefficients for a vanishing convective flux over the particle surface.

Gasification of biomass or coal and their derivatives occurs predominantly in and on a porous particle. It is assumed to have a network of pores with a certain size distribution. The pores may be connected interchangeably or may end with no connection to neighbouring pores. A network of pores increases the inner surface significantly giving the reactants a much larger access to undergo conversion with the solid matrix labelled also heterogeneous or intrinsic reaction. In a heterogeneous reaction the reactants diffuse to the pore surface and adsorb onto it due to chemical bonds. After reaction is completed, the formed products desorb from the surface and diffuse through the pore space to the outer surface. Hence, the process of heterogeneous reaction may be divided into the following steps:

- diffusion of one or more reactants through the pore space onto the pore surface;
- adsorption of reactants on the pore surface;
- chemical reaction and formation of products;
- desorption of the products from the pore surface;
- diffusion of one or more products through the pore space to the outer surface.

In this sequence, the overall rate of the entire process is determined by the slowest of these steps. Usually, the reaction process is rate-limiting at low temperatures. However, diffusion appears to be rate-limiting due to insufficiently provided reactants at higher temperatures. In both cases the solid matrix is reduced on the inner pore surface. This in general leads to an increased porosity. If conversion takes place within the entire volume of the particle, usually no change in volume is observed as in the case for a reacting core mode. However, if conversion is confined to the outer surface of a particle pore openings expand and eventually grow together, and thus, making the particle recess. Conversion occurring either within a particle or on the outer surface only is determined by the ratio between a chemical τ_R and a diffusion τ_D time scale, that is expressed by the Thiele modulus. The effectiveness factor, derived from the Thiele modulus Th or the second Damköhler number Da_2 , represents the ratio between the reactions taking place on the inner particle surface and the outer surface. These dimensionless numbers are defined as

$$Th = Da_2 = \frac{kS_i}{D/r^2} = \frac{1/\tau_R}{1/\tau_D} \quad (10)$$

$$\eta = \frac{1}{3Th} (3\sqrt{Th} \coth 3\sqrt{Th} - 1) \quad (11)$$

with k , S_i , r and D denoting the Arrhenius coefficient, inner surface, representative length and diffusion coefficient, respectively. The effectiveness factor versus Thiele modulus is depicted in Fig. 1 for different geometries.

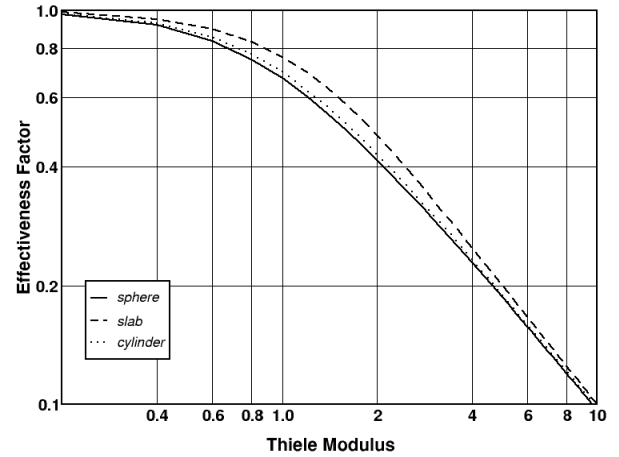


Fig. 1 Effectiveness factor versus Thiele modulus

For a Thiele modulus smaller than 1, diffusive transport is faster than conversion, so that a reaction takes place within almost the entire particle volume yielding an effectiveness higher than 70%. However, for a Thiele modulus larger than 1, the reaction rate is larger than diffusion, so that reactants are converted near the outer surface. Hence, no reactants remain to diffuse into the interior part of a particle, and thus representing the shrinking core mode. Increasingly small fractions of the inner surface are involved into the reaction process leading to a reduced effectiveness. Hence, in the shrinking core mode, depleted material correlates with an appropriate geometrical recession of the particle, which is adopted in the current study. This allows estimating a shrinkage without empirical pa-

rameters and changing between the two modes dependent on the heat and mass transfer conditions as encountered in a moving bed of solid particles. Thus, depletion of solid fuel material in the outermost cell is converted into a reduction of particle volume e.g. radius as shown in Fig. 2. This procedure would lead to a vanishing cell size, and eventually to numerical undefined behaviour. Therefore, the present approach includes a remeshing that generates cells with appropriate sizes for stable numerical behaviour as depicted at in Fig. 2.

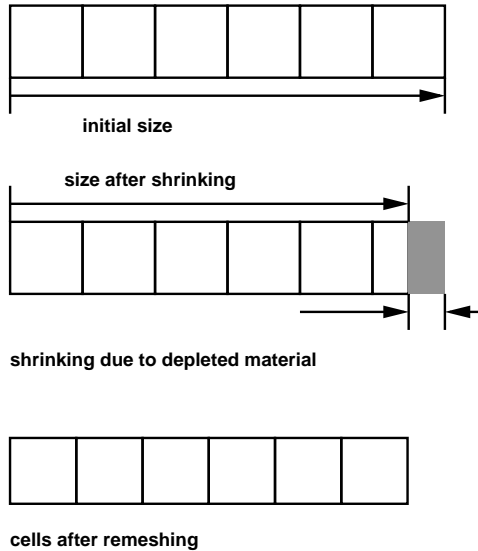


Fig. 2 Reduction in size of a particle due to shrinking

Although the lines for flat, long cylindrical and spherical particles in Fig. 1 cover a wide range of volume-to-surface ratios, the difference in effectiveness factors turns out to be moderate, thus justifying the assumption that a spherical geometry can represent reasonably well various shapes. Further evidence for this behaviour is provided by the experimental investigations of Senf [46]. His results indicate that the PM (particulate matter) emissions and volume to surface ratios are not correlated. However, in order to take account for these geometries, the differential conservation equations are expressed in Cartesian, cylindrical and spherical reference systems.

3. Results

This section presents validation of the model for gasification of char with an emphasis on a recessing volume. Experiments were carried out by Schäffer and Wyrsh [47] for spherical char particles of 10 and 15 mm in diameter. Further parameters employed for the simulation are listed in Table 1.

Material properties employed for the predictions are listed in Table 2. Kinetics for char gasification were described by the data of Kulasekaran et al. [48], which yielded a good agreement between measured and predicted data as shown in Fig. 3. In both cases particle mass reduces with an asymptotic character due to a shrinking surface. It causes increasingly aggravating mass transfer conditions due to a reduction that decreases the amount of available reactants on the outer surface of a particle. Hence, reaction rates decrease as depicted in Fig. 4. A maximum conversion rate is reached shortly after light-off that then contin-

uously decreases due to a recessing surface for mass transfer.

Table 1

Simulation parameters

Parameter	Value
Initial temperature	300 K
Initial oxygen density	0.232 kg/m ³
Heating temperature	773 K
Ambient oxygen density	0.232 kg/m ³
Heat transfer coefficient	40 W/Km ²
Mass transfer coefficient	0.015 m/s

Table 2

Material properties of char

Property	Value
Particle diameter	10.0/15.0 mm
Molecular weight	12 kg/kmol
Density	150 kg/m ³
Specific heat capacity	420.0 J/(kgK)
Diffusion coefficient	10 ⁻⁵ m ² /s
Heat conduction	0.1 W/(mK)
Porosity	0.85
Specific inner surface	34000.0 m ⁻¹
Pore length	10 ⁻⁴ m

Due to the high reactivity of the char, the domain of reaction is limited to a small region near the outer surface which indicates clearly a shrinking core regime. As pointed out in the previous section, the reacting core and shrinking core regimes were distinguished by the Thiele modulus, i.e., the second Damköhler number.

If the Damköhler number exceeds a value of 1, recession of the outer surface is taken into account. Fig. 5 depicts the evolution of the Damköhler number versus time and space during gasification of a char particle of 10 mm diameter.

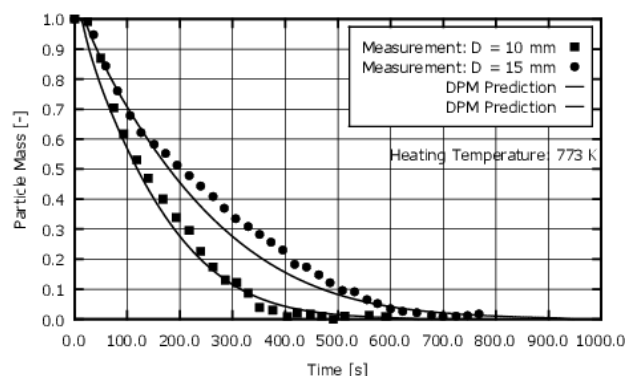


Fig. 3 Comparison between measurements and predictions for gasification of char particles of 10 mm and 15 mm diameter

For most of the gasification period of ~700 s, the Damköhler number exceeds well the value of 1. It indicates clearly that reactions proceed much faster than transport of reactants, e.g., oxygen. Reactants that are provided by mass transfer onto the outer surface of a char particle are consumed immediately due to a high reaction rate. Hence, no reactants remain to diffuse into interior parts of

a particle, so that there no further reaction takes place. Additionally, the profile of the Damköhler number in Fig. 5 shows a declining characteristics versus time, which represents quite accurately the physical behaviour. Due to a recessing surface, i.e., decreasing distances to be bridged by diffusion, the particle gives easier access to its interior for reactants, so that the Damköhler number decreases.

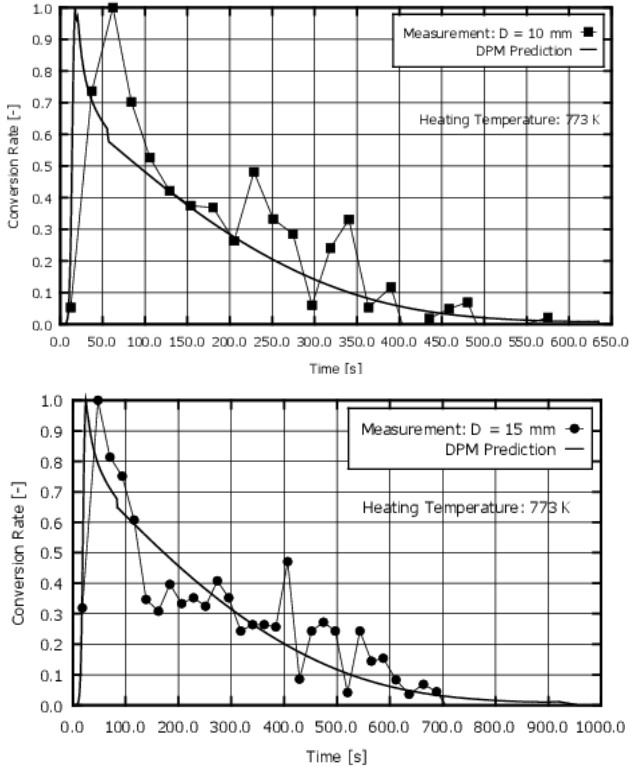


Fig. 4 Comparison between experimental and predicted conversion rates for particles of diameter 10 mm (top) and 15 mm (bottom)

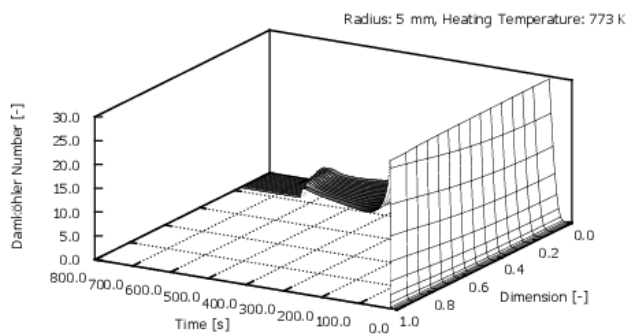


Fig. 5 Damköhler number versus time and space during gasification of a char particle of 10 mm diameter

The same characteristics are also encountered during the initial stage of gasification as shown in Fig. 6. Fig. 6 is a magnification of Fig. 5 during the initial period of gasification of 40 s. Heating of the particle starts at an initial temperature of 300 K with a slowly increasing temperature versus time. The reaction rates vanish at low temperature, so that no conversion of reactants takes place and they diffuse towards the centre of the particle. This corresponds to an effectiveness of almost 100% at Damköhler numbers below 1 representing reacting core behaviour. With rising temperatures the reaction rate increases and, consequently, reaches Damköhler numbers above 1 indi-

cating shrinking core behaviour. A procedure that detects shrinking and reacting core behaviour is important for predictions of particle gasification under varying heat and mass transfer conditions, as encountered on grates at which the current approach aims [49, 50]. In order to emphasise the impact of particle shrinking, gasification was also predicted excluding shrinkage as shown in Fig. 7.

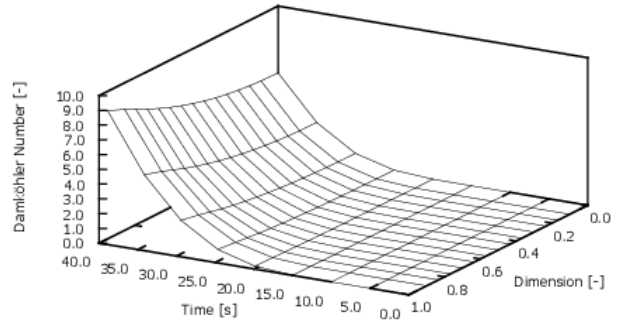


Fig. 6 Damköhler number versus time and space during initial gasification of a char particle of 10 mm diameter

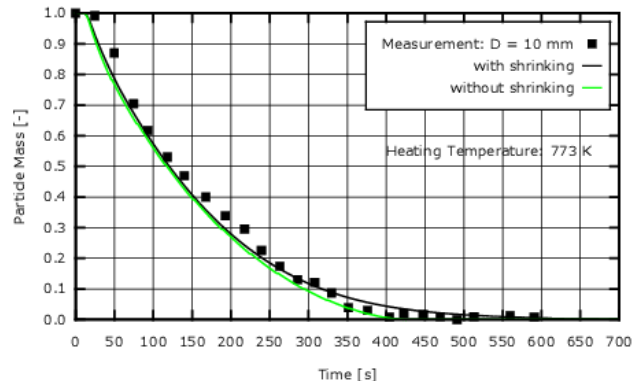


Fig. 7 Comparison between measurements and predictions during gasification of a char particle of 10 mm diameter with the effect of shrinking

Only vanishing differences for the mass loss of the char particle occur during the initial gasification period because a recession of the particle surface is also very small. After a period of ~ 250 s the profiles start deviating until gasification without shrinking ends at ~ 400 s. Since the outer surface does not decrease, heat and mass transfer is not aggravated as is the case for a recessing surface. This provides more oxygen for gasification, and thus, reduces the gasification period. In the case of a recessing surface, mass transfer of reactants decreases, so that the reaction rate reduces, and therefore, gasification comes to an end at ~ 650 s. This attributes to a difference of $\sim 33\%$ for the gasification period, and effects significantly predicted residence times in reactors. Fig. 8 depicts the oxygen profile versus time and space during gasification of a char particle of 10 mm diameter. The distribution of oxygen in space is clearly dependent on the ratio of transport to reaction time scales. For low Damköhler numbers, oxygen still penetrates the particle due to low reaction rates during an initial stage of gasification. This characteristic correlates well with the distribution of the Damköhler number in Fig. 6.

With rising temperatures, oxygen provided through external mass transfer is consumed in a region close to the outer surface, so that no reactants remain to

penetrate the interior of the particle, as shown in Fig. 8. A magnification of the oxygen profile during part of the gasification period as depicted in Fig. 9 shows a steep gradient near the outer surface of the particle, and thus confirms the shrinking core mode as the prevailing mechanism for particle conversion.

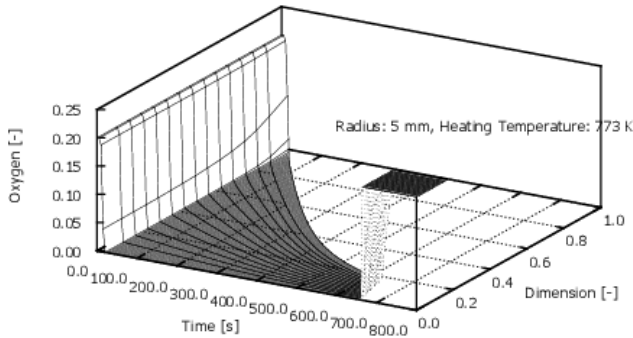


Fig. 8 Oxygen profile during gasification of a char particle of 10 mm diameter

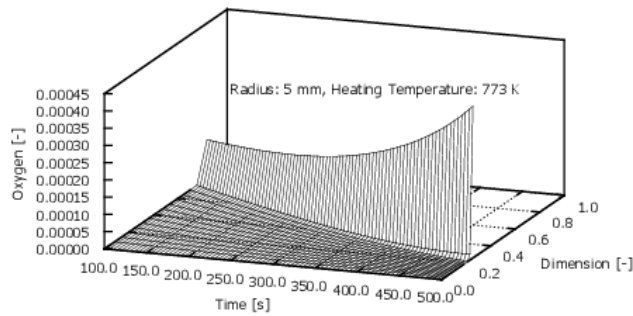


Fig. 9 Magnification of oxygen profile during gasification of a char particle of 10 mm diameter

Fig. 10 depicts the corresponding temperature distribution versus time and space during gasification of a char particle of 10 mm diameter. During the initial phase the increasing temperature is determined by ambient heat transfer with a heating temperature of 773 K. Once, the ignition temperature is exceeded, the temperature rises again due to heat release from partial oxidation of char with available oxygen. While the particle is shrinking, less and less mass has to be heated, so that the heat released during gasification causes a steep increase in temperature at a time of app. 600 s. At this stage, char is depleted and hereafter the temperature decreases exponentially by heat transferred to the ambient.

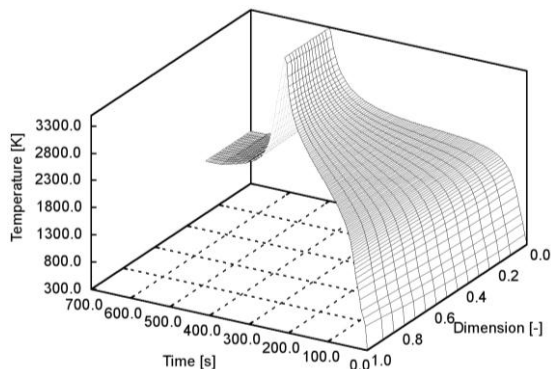


Fig. 10 Temperature profile during gasification of a char particle of 10 mm diameter

These characteristics are also to be observed for the char profile versus time and space in Fig. 11. A depletion of char takes place within the entire particle during an initial stage of gasification due to low Damköhler numbers. Eventually, Damköhler numbers rise above a value of 1, so that the shrinking core behaviour prevails. Within this regime, solid material is converted only close to the outer surface, whereas no conversion occurs within the particle.

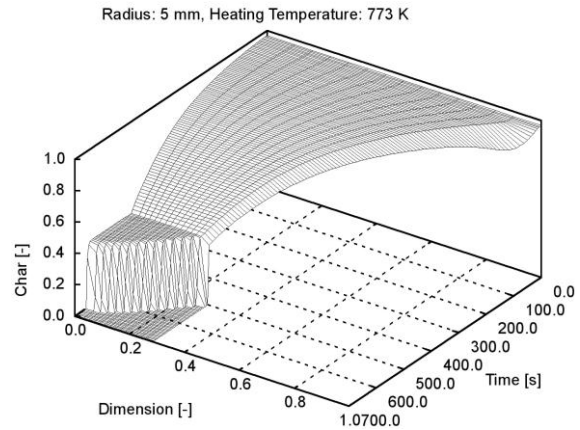


Fig. 11 Char profile during gasification of a char particle of 10 mm diameter

4. Summary

The current contribution presented a numerical approach to describe gasification of solid char particles including a recessing surface. It includes one-dimensional and transient differential conservation equations for mass, momentum, species and energy. The conservation equations are discretised by the finite volume method and the resulting algebraic equations are solved by standard linear solvers. Additionally, shrinking of particles during gasification is taken into account. A reacting core and shrinking core behaviour is distinguished by the second Damköhler number that represents a ratio between a diffusion and reaction time scale. For Damköhler numbers below 1, the model assumes a reacting core behaviour, whereas a shrinking core behaviour is predicted for Damköhler numbers larger than 1. Thus, the model is independent of empirical correlations and employs the appropriate behaviour depending on physical characteristics. This is important for a large number of engineering devices such as combustion on forward or backward acting grates. There, particles experience different conditions depending on their position of the grate, for which the current approach is developed. A comparison between measurements and predictions for gasification of differently sized char particles showed good agreement. Additional predictions excluding the effect of shrinkage indicated that the gasification period was underestimated by ~33% under the conditions considered.

Appendix A. Error Analysis

The accuracy of the predicted results, in particular correlation between measured data and predicted results, is addressed in the following section. As mentioned above, kinetic data from literature was applied to predict gasification of coke material. In order to estimate the quality of the predicted results in comparison to the measurements, the

Pearson product-moment correlation coefficient, sometimes referred to as the PMCC, and typically denoted by r , was employed. The Pearson product-moment correlation coefficient for two samples x and y , of sizes n , is expressed as follows

$$\begin{aligned} \text{Kor}_e(x, y) &= \rho_e(x, y) = r_{xy} = \\ &= \frac{\sum_{i=1}^n (x_i - \bar{x})(y_i - \bar{y})}{\sqrt{\sum_{i=1}^n (x_i - \bar{x})^2} \sqrt{\sum_{i=1}^n (y_i - \bar{y})^2}} \end{aligned} \quad (\text{A.1})$$

where $\bar{x} = \frac{1}{n} \sum_{i=1}^n x_i$ and $\bar{y} = \frac{1}{n} \sum_{i=1}^n y_i$ denote the statistical means of x and y , respectively. Applying this correlation to the measured and predicted data shown in Fig. 3 gives correlation coefficients for the differently sized particles as listed in Table A.1 that is perceived as a very good correlation. It supports also the argument that carefully evaluated kinetic data in conjunction with an accurate model represents the physical-chemical behaviour with high quality. A similar assessment for the conversion rate in Fig. 4 was not carried out, because the rate was obtained by forward-differencing the measured data of Fig. 3. It is a rather crude approach to estimate the rate, and therefore, can only be treated as a rough assessment and is compared to predicted data in terms of general trends.

Table A.1

Pearson product-moment correlation coefficients for experimental and theoretical data based on the presented model

Particle diameter	Correlation coefficient
10.0 mm	0.9978
15.0 mm	0.9936

References

1. **Sciazko, M.; Zuwała, J.; Pronobis, M.; Winnicka, G.** 2007. Problems related to combustion of biomass in energy-producing boilers, *Ins. Chem. Przerobki Wegla i Pol Sl., Zabrze, Poland* (in Polish).
2. **VanLith, S.C.** 2005. Release of Inorganic Elements during Wood-firing on a Grate. PhD thesis, Technical University of Denmark, Denmark.
3. **Valmari, T.** 2000. Potassium behaviour during combustion of wood in circulating fluidised bed power plants. PhD thesis, Technical Research Centre of Finland, Finland.
4. **Misra, M.K.; Ragland, K.W.; Baker, A.J.** 1993. Wood ash composition as a function of furnace temperature, *Biomass Bioenergy* 4: 103-116. [http://dx.doi.org/10.1016/0961-9534\(93\)90032-Y](http://dx.doi.org/10.1016/0961-9534(93)90032-Y).
5. **Simmons, W.W.** 1983. Analysis of a single particle wood combustion in convective flow. PhD thesis, University of Wisconsin-Madison, USA.
6. **Chan, W.R.; Kelbon, M.; Krieger B.B.** 1985. Modeling experimental verification of physical chemical processes during pyrolysis of a large biomass particle, *Fuel* 64: 1505-1513. [http://dx.doi.org/10.1016/0016-2361\(85\)90364-3](http://dx.doi.org/10.1016/0016-2361(85)90364-3).
7. **Alves, S.S.; Figueiredo, J.L.** 1989. A model for pyrolysis of wet wood, *Chem. Eng. Sci.* 44: 2861-2869. [http://dx.doi.org/10.1016/0009-2509\(89\)85096-1](http://dx.doi.org/10.1016/0009-2509(89)85096-1).
8. **Saastamoinen, J.J.** 1994. Model for drying pyrolysis in an updraft biomass gasifier. In: Bridgewater A.V., editor, *Advances in Thermochemical Biomass Conversion*, 186-200.
9. **Gronli, M.** 1996. A theoretical experimental study of the thermal degradation of biomass. PhD thesis, The Norwegian University of Science Technology, Trondheim, Norway.
10. **Peters, B.** 1999. Classification of combustion regimes in a packed bed based on the relevant time and length scales, *Combustion Flame* 116: 297-301. [http://dx.doi.org/10.1016/S0010-2180\(98\)00048-0](http://dx.doi.org/10.1016/S0010-2180(98)00048-0).
11. **Bryden, K.M.; Ragland, K.W.; Rutland, C.J.** 2002. Modelling thermally thick pyrolysis of wood, *Biomass & Energy* 22: 41-53.
12. **Maa, P.S.; Bailie, R.C.** 1973. Influence of particle sizes environmental conditions on high temperature pyrolysis of cellulosic material. I (theoretical), *Combustion Science Technology* 7: 257-269. <http://dx.doi.org/10.1080/00102207308952366>.
13. **Villiermaux, J.; Antoine, B.; Lede, J.; Soullignac, F.** 1986. A new model for thermal volatilisation of solid particles undergoing fast pyrolysis, *Chemical Engineering Science* 41: 151-157. [http://dx.doi.org/10.1016/0009-2509\(86\)85208-3](http://dx.doi.org/10.1016/0009-2509(86)85208-3).
14. **Parker, W.J.** 1988. Prediction of heat release rate of wood. PhD thesis, George Washington University.
15. **Saastamoinen, J.; Richard, J.** 1988. Drying, pyrolysis and combustion of biomass particles, *Research in Thermochemical Biomass Conversion* 1: 221-235. http://dx.doi.org/10.1007/978-94-009-2737-7_18.
16. **Ragland, K.W.; Boeger, J.C.; Baker, A.J.** 1988. Model of chunkwood combustion, *Forest Products J.* 38: 27-32.
17. **Ouedraogo, A.; Mulligan, J.C.; Cleland, J.G.** 1998. A quasi-steady shrinking core analysis of wood combustion, *Combustion Flame* 114: 1-12. [http://dx.doi.org/10.1016/S0010-2180\(97\)00291-5](http://dx.doi.org/10.1016/S0010-2180(97)00291-5).
18. **Di Blasi, C.** 1996. Heat, momentum mass transport through a shrinking biomass particle exposed to thermal radiation, *Chem. Eng. Sci.* 51: 1121-1132.
19. **Hagge, M.J.; Bryden, K.M.** 2002. Modeling the impact of shrinkage on the pyrolysis of dry biomass, *Chem. Eng. Sci.* 57: 2811-2823. [http://dx.doi.org/10.1016/S0009-2509\(02\)00167-7](http://dx.doi.org/10.1016/S0009-2509(02)00167-7).
20. **Tran, H.C.; White, R.H.** 1992. Burning rate of solid wood measured in a heat release rate calorimeter, *Fire Materials* 16: 151-157. <http://dx.doi.org/10.1002/fam.810160406>.
21. **Chapman, P.** 1996. CFD enhances waste combustion design modification, In: *Combustion Canada 1996*, Ottawa, Ontario, Canada, June 5 - 7, 1996.
22. **Rogers, J.E.L.; Sarofim, A.F.; Howard, J.B.; Williams, G.C.; Fine, D.H.** 1975. Combustion characteristics of simulated shredded refuse, 15th Symposium (International) on Combustion 15: 1137-1148.
23. **Hellwig, M.** 1988. Zum Abbrand von Holzbrennstoffen unter besonderer Berücksichtigung der zeitlichen Abläufe. PhD thesis, Technische Universität München, Germany.

24. **Kansa, E.J.; Perlee, H.E.; Chaiken, R.F.** 1977. Mathematical model of wood pyrolysis including internal forced convection, *Combustion Flame* 29: 311-324. [http://dx.doi.org/10.1016/0010-2180\(77\)90121-3](http://dx.doi.org/10.1016/0010-2180(77)90121-3).
25. **Man, Y.H.; Byeong, R.C.** 1994. A numerical study on the combustion of a single carbon particle entrained in a steady flow, *Combustion Flame* 97: 1-16.
26. **Lee, J.C.; Yetter, R.A.; Dryer, F.L.** 1995. Transient numerical modelling of carbon ignition and oxidation. *Combustion Flame* 101: 387-398. [http://dx.doi.org/10.1016/0010-2180\(94\)00207-9](http://dx.doi.org/10.1016/0010-2180(94)00207-9).
27. **Lee, J.C.; Yetter, R.A.; Dryer, F.L.** 1996. Numerical simulation of laser ignition of an isolated carbon particle in quiescent environment, *Combustion Flame* 105: 591-599. [http://dx.doi.org/10.1016/0010-2180\(96\)00221-0](http://dx.doi.org/10.1016/0010-2180(96)00221-0).
28. **Rattee, J.; Mariasb, F.; Vaxelaireb, J.; Bernada, P.** 2009. Mathematical modelling of slow pyrolysis of a particle of treated wood waste, *Journal of Hazardous Materials* 170: 1023-1040. <http://dx.doi.org/10.1016/j.jhazmat.2009.05.077>.
29. **Specht, E.** 1993. Kinetik der Abbaureaktionen. Habilitationsschrift, TU Clausthal-Zellerfeld.
30. **Laurendeau, N.M.** 1978. Heterogeneous kinetics of coal char gasification combustion, *Progr. Energy Combust. Sci.* 4: 221-270.
31. **Elliott, M.A.** 1981. Chemistry of Coal Utilization, chapter: Fundamentals of Coal Combustion, p. 1153. Wiley, New York., Suppl. vol. 2.
32. **Blevins, R.D.** 1984. Applied Fluid Dynamics Handbook. Krieger Publishing Company, Malabar, Florida.
33. **Seebauer, V.; Petek, J.; Staudinger, G.** 1997. Effects of particle size, heating rate pressure on measurement of pyrolysis kinetics by thermogravimetric analysis, *Fuel* 76: 1277-1282. [http://dx.doi.org/10.1016/S0016-2361\(97\)00106-3](http://dx.doi.org/10.1016/S0016-2361(97)00106-3).
34. **Pai Shih-I.** 1977. Two-Phase Flows. Vieweg Tracts in Pure Applied Physics, Braunschweig.
35. **Dullien, F.A.L.** 1979. Porous Media Fluid Transport Pore Structure. Academic Press, San Diego.
36. **Aho, M.** 1987. Pyrolysis combustion of wood peat as a single particle a layer. VTT Report, 465.
37. **Saastamoinen, J.; Aho, M.; Linna, V.L.** 1993. Simultaneous pyrolysis char combustion, *Fuel* 72: 599-609. [http://dx.doi.org/10.1016/0016-2361\(93\)90571-I](http://dx.doi.org/10.1016/0016-2361(93)90571-I).
38. **Saastamoinen, J.; Haukka, P.** 1998. Simultaneous drying pyrolysis in fixed bed, combustion of wet biomass, 11th International Drying Symp., Halkidiki, Greece, p. 1975-1982.
39. **Saastamoinen, J.; Richard, J.-R.** 1998. Simultaneous drying pyrolysis of solid fuel particles, *Combustion Flame* 106: 288-300. [http://dx.doi.org/10.1016/0010-2180\(96\)00001-6](http://dx.doi.org/10.1016/0010-2180(96)00001-6).
40. **Peters, B.** 1997. Numerical simulation of heterogeneous particle combustion accounting for morphological changes, In: 27th International Conference on Environmental Systems, Lake Tahoe, USA, July 14-17, 1997, SAE-paper 972562.
41. **Bird, R.B.; Stewart, W.E.; Lightfoot, E.N.** 1960. Transport Phenomena. John Wiley & Sons.
42. **Botterill, J.S.M.** 1975. Fluid-Bed Heat Transfer. Academic Press.
43. **Bejan, A.** 1984. Convection Heat Transfer. John Wiley & Sons.
44. **Grigull, U.** 1963. Die Grundgesetze der Wärmetübertragung. Springer Verlag.
45. **Brauer, H.** 1971. Stoffaustausch einschließlich chemischer Reaktionen. Verlag Sauerländer.
46. **Senf, N.** 1996. Low emissions residential cordwood combustion in high mass appliances – recent research results. In: Combustion Canada 1996, Ottawa, Ontario, Canada, June 5-7, 1996.
47. **Schäer, B.; Wyrsh, F.** 2000. Untersuchungen der Produktzusammensetzung bei thermochemischen Konversionsprozessen von Biomasse. Diplomarbeit, ETH Zürich, Institut für Energietechnik, LTNT.
48. **Kulasekaran, S.; Linjewile, T.; Agarwal, P.; Biggs, M.** 1998. Combustion of porous char particle in an incipiently fluidized bed, *Fuel* 77: 1549-1560. [http://dx.doi.org/10.1016/S0016-2361\(98\)00091-X](http://dx.doi.org/10.1016/S0016-2361(98)00091-X).
49. **Peters, B.; Frey, H.; Hunsinger, H.; Vehlow, J.** 2003. Characterisation of municipal solid waste combustion in a grate furnace, *Waste Management* 23(8): 689-701. [http://dx.doi.org/10.1016/S0956-053X\(02\)00070-3](http://dx.doi.org/10.1016/S0956-053X(02)00070-3).
50. **Peters, B.; Džiugys, A.; Hunsinger, H.; Krebs, L.** 2005. An approach to qualify the intensity of mixing on a forward acting grate, *Chem. Eng. Sci.* 60(6): 1649-1659. <http://dx.doi.org/10.1016/j.ces.2004.11.004>.

B. Peters, A. Džiugys, R. Navakas

KIETO KURO DALELIŲ MAŽĖJIMO
DUJOFIKAVIMO METU MODELIS, PAGRĪSTAS
PERNAŠOS IR REAKCIJŲ LAIKO MASTELIAIS

R e z i u m ė

Straipsnyje pateikiamas dalelių mažėjimo modelis, vykstant anglinės liekanos, susidariusios biomasės arba anglies pirolizės metu, dujofikavimui. Modelis, aprašantis anglinės dalelės dujofikavimą, pagrįstas vienmatėmis diferencialinėmis masės, judesio kiekio, cheminio junginio koncentracijos ir energijos tvermės lygtimis. Dalelės dydžio mažėjimas įvertinamas fizikiniu pagrindu, naudojant Tilės (Thiele) modulį arba antrąjį Damkiolerio (Damköhler) skaičių, kuris aprašo santykį tarp difuzijos ir reakcijos laikų ir pirmiausia leidžia atskirti reaguojančio ir besitraukiančio dalelės branduolio elgseną. Tokiu būdu, šiam modeliui nereikalingos empirinės koreliacijos. Modelis pritaikytas kietųjų dalelių reaguojančiam sluoksniui. Esant reaguojančio branduolio režimui, kietosios medžiagos apimtį sumažėjimas padidina dalelės kietosios matricos porėtumą, tuo tarpu traukiantis branduoliui, mažėja tūris.

B. Peters, A. Džiugys, R. Navakas

A SHRINKING MODEL FOR
COMBUSTION/GASIFICATION OF CHAR BASED ON
TRANSPORT AND REACTION TIME SCALES

S u m m a r y

The objective of this contribution is to introduce a shrinking model for gasification of char formed by pyrolysis of biomass or coal. The model describing gasification

of a charred particle is based on one-dimensional and transient differential conservation equations for mass, momentum, species and energy. Shrinkage is estimated by a physically based approach of the Thiele modulus or second Damköhler number. It represents a ratio of diffusion time to reaction time and primarily allows distinguishing between a reacting and shrinking core behaviour. Thus, this approach does not require any empirical correlations and is employed to a reacting bed of solid particles. Within the

reacting core domain, depleted solid material increases porosity of the solid matrix, while the shrinking core behaviour contributes to a recessing volume.

Keywords: thermal conversion, solid fuel, packed bed, model.

Received April 05, 2011

Accepted March 29, 2012